Environmental Science and Pollution Research (2023) 30:20923–20933
https://doi.org/10.1007/s11356-022-23684-4

RESEARCH ARTICLE

Photosynthetic regulation in response to strontium stress in moss *Racomitrium japonicum* L

Hui Ren[1] · Renhua Huang[2] · Ying Li[4] · Wanting Li[1] · Liuliu Zheng[1] · Yanbao Lei[3] · Ke Chen[1]

Received: 8 July 2022 / Accepted: 12 October 2022 / Published online: 20 October 2022

Abstract

Strontium (Sr^{2+}) pollution and its biological effects are of great concern including photosynthetic regulation, which is fundamental to environmental responses, especially for bryophytes during their terrestrial adaptation. Alternative electron flows mediated by flavodiiron proteins (FLVs) and cyclic electron flow (CEF) in photosystem I (PSI) are crucial to abiotic stresses moss responses; however, little is known about the moss photosynthesis regulation under nuclide treatment. We measured chlorophyll fluorescence parameters in PSI, photosystem II (PSII) and the P700 redox state, oxidative stress in the moss *Racomitrium japonicum* under low (5 mg/L), moderate (50 mg/L) and high (500 mg/L) Sr^{2+} stress level. Moderate and high Sr^{2+} stress triggered H_2O_2 and malondialdehyde (MDA) generation, and catalase (CAT) activity increases, which are involved in reactive oxygen species regulation. The significant PSII photochemistry (Fv/Fm), Chla/chlb, Y(I)/Y(II), Y(NA), Y(ND) and ETRI-ETRII decreases at moderate and high Sr^{2+}, and the Y(I), Y(II) decreases at high Sr^{2+} revealed the photo-inhibition and photo-damage in PSI and PSII by moderate and high Sr^{2+} stress. The nonphotochemical quenching (NPQ) increased significantly at moderate and high Sr^{2+} stress, reflecting a heat-dissipation-related photo-protective mechanism in antenna system and reaction centers. Moreover, rapid re-oxidation of P700 indicated that FLV-dependent flows significantly regulated PSI redox state under moderate and high Sr^{2+} stress. and CEF upregulation was found at low Sr^{2+}. Finally, photosynthetic acclimation to Sr^{2+} stress in *R. japonicum* was linked to FLVs and CEF adjustments.

Keywords Sr^{2+} stress · Cyclic electron transport · Flayodiiron proteins · Photosynthetic acclimation

Introduction

During the development and utilization of nuclear energy, many radionuclides can enter the natural environment (Choppin 2007). Surrounding plants growth is inevitably exposed to nuclide stress. Increasing concentration of nuclides pollution induce a series of changes in plants, impacting photosynthesis (Maksimovic et al. 2014). In the process of adapting to the environment stress, plants were capable of adsorbing the nuclides from environment to make it possible for bioremediation (Wang et al. 2017). But when the nuclide concentration reaches the plant body clearance limit, stress pressures are manifested in chlorophyll content reductions, which affect the chloroplast absorption and transmission of light energy, thereby reducing the maximum photochemical efficiency (F_v/F_m), and the absorption and utilization of light energy by photosystem II(PSII) (Li et al. 2013). The photosynthetic electron transport process is blocked, the excess excitation energy increases and the plants are forced to release this PSII-absorbed excessive

Responsible Editor: Gangrong Shi

Hui Ren and Renhua Huang contributed equally to this work.

✉ Ke Chen
chenke@swust.edu.cn

[1] School of Life Science and Engineering, Southwest University of Science and Technology, Mianyang 621010, China

[2] Hubei Engineering Research Center for Specialty Flowers Biological Breeding, Jingchu University of Technology, Jingmen 448000, Hubei, China

[3] China-Croatia "Belt and Road" Joint Laboratory On Biodiversity and Ecosystem Services, CAS Key Laboratory of Mountain Ecological Restoration and Bioresource Utilization & Ecological Restoration and Biodiversity Conservation Key Laboratory of Sichuan Province, Chengdu Institute of Biology, Chinese Academy of Sciences, Chengdu 610041, China

[4] Administration Bureau of Jiuzhaigou National Nature Reserve, Jiuzhaigou 623402, China

energy through non-radiative thermal dissipation (Luo et al. 2011). Cheng et al. (2022a) found that strontium ions (0.2–6 mM) had effect on light energy conversion and utilization in A. tricolor. Strontium stress can increase the excess light energy in the plants, resulting in the accumulation of QA − and block in QB downstream of the electron transfer chain in PSII, leading to the acceptor side of PSII being more vulnerable to strontium stress than the donor side. In a large number of nuclide studies, cesium stress spiked in solution inhibited performance of PSII via drop of effective quantum yield of PSII photochemistry (φPSII) and photochemical quenching of chlorophyll fluorescence, increase of nonphotochemical quenching (NPQ), block in electron transfer process beyond QA, decline of electron transport activity (ETo/RC, ψo and φEo) and restraint of P700 reduction (WIP) (Cheng et al. 2022b). Furthermore, due to decreased photosynthetic performance, the maximum relative electron transfer rate (ETR_{max}) decreases (Li et al. 2013); when absorbing the same photoelectrons, CO_2 fixation slowed down during the photosynthetic electron transfer of plants under stress and the NADPH produced cannot be consumed immediately, leading to a decrease in the $NADP^+$/NADPH ratio. The lack of $NADP^+$ induces excited states and reactive oxygen species production within PSI (Yamamoto et al. 2016; Yamamoto and Shikanai 2019; Huang et al. 2019a). Furthermore, the reactive oxygen species produced within PSI cannot be immediately scavenged by the antioxidant system, leading to oxidative damage to PSI (Takagi et al. 2016). With PSI photoinhibition, both linear electron flow (LEF) and cyclic electron transport (CEF) are depressed, which decreases photosynthetic CO_2 assimilation rate and impairs plant growth (Brestic et al. 2015, 2016; Shimakawa and Miyake 2019; Zivcak et al. 2015; Yamori et al. 2016).

Plants produce protective responses when experiencing external stresses, for example, photosynthetic organisms have evolved with a complex mechanism to repair PSII (Alboresi et al. 2019). Biological stress caused by environmental deterioration usually reduces the maximum photosynthetic capacity of the plants. Hence, nuclide concentration increases reduce plant photosynthesis, affects and aggravates the stress of excess light (Li et al. 2009), and inhibits linear electron flow (LEF) and circulating electron transmission (CEF). During NADPH and ATP producing water cracking in PSII, ΔpH-dependent electron transfers actively regulated the activity of PSII (Tikkanen et al. 2014) and suppressed electron transfer and excessive ΔpH, inducing nonphotochemical quenching (NPQ) to consume excessive light quanta in PSII to reduce photoinhibition in PSII (Tan et al. 2020a). Therefore, photochemical quenching is instrumental to protect the optical system II from excess electrons (Tikkanen et al. 2014). Studies in numerous plants and algae also showed that when assimilation reaction of light-absorption exceeds the light utilization capacity, a photosynthetic light capture regulation (qE) is triggered, which scattered the excess absorbed light energy in the form of thermal dissipation and initiated the photosynthetic protection device in the time scale of minutes (Li et al. 2009).

Although photosynthetic organisms have evolved a protective strategy for the repair of PSII-induced photodamage (Alboresi et al. 2019), PSI is inevitably affected by the balance between PSII damage and repair, caused as external stress intensifies (Meng 2013). PSI is difficult to recover after damage, and its effect is more significant than that of PSII (Alboresi et al. 2019). To prevent photosystem inhibition and damage, the production and consumption of ATP and NADPH must be balanced (Walker et al. 2014). Early studies of *Arabidopsis* model plants revealed that differences between ATP and NADPH could be balanced by CEF around the PSI. In CEF, electrons from NADPH circle the PSI into the plastome quinone pool, providing additional ATP without reducing $NADP^+$ and increasing ATP and NADPH production to maintain their equilibrium. Therefore, the protective effect of CEF on PSI is inestimable (Strand et al. 2015; Tan et al. 2020a; Walker et al. 2014). In bryophytes, CEF and flavodiiron proteins (FLV) are active, and these two circulatory mechanisms play a synergistic role in protecting light and organs from excessive reduction (Lu 2008; Storti et al. 2019).

Light damage caused by environmental stress is usually harmful to PSI; however, the CEF around PSI was found to be critical to the PSI photoprotection (Yang et al. 2019). With high light stimulation, CEF is rapidly activated in *Arabidopsis thaliana* and *Bletilla striata*, which contributes to the rapid formation of ΔpH and additional ATP to compensate for the difference between ATP/NADPH and primary metabolism in LEF, accepts electrons from PSI, preventing P700 over reduction and ROS protection in PSI, thus protecting the donor and receptor side PSI (Yang et al. 2019). Interestingly, excessive photo-stress caused by ambient pressure can lead to excessive reduction of PSI electron carrier (Li et al. 2009; Yang et al. 2019). At this point, brass diferrin-mediated alternative electron flow activity is more prominent in algae and bryophyte, and FLV action can partially compensate for the transmission of loop electrons, thus reducing damage from receptor-side electron accumulation (Storti et al. 2019). These kinetic analyses reveal the critical role of CEF and FLV in plant photoprotection; however, little is known about CEF and FLV activity kinetics in non-angiosperms following nuclide stimulation.

Estimated to the external environment, plant photosynthesis becomes more sensitive; for example, Chernobyl event impacted plant photosynthesis considerably (Paatero et al. 1998). Previous research has reported that bryophytes adsorb heavy metals by developing adsorption models (Chen 2007; Marešová et al. 2011). As for plant tolerance to radionuclides, the response of the photoprotection mechanism

partially contributes to the potential detoxification mechanism (Lai and Luo 2019; Maksimovic et al. 2014). Due to plant stresses, the photosynthetic chrome concentration decreases, and the photosynthesis intensity decreases. To relieve the pressure of the optical system, the body stimulates circulating electron transfer around the PSI, provides ΔpH for CO_2 assimilation, promotes the efficient operation of photochemical reaction and reduces electron accumulation in PSI; CEF participates in NPQ induction to ΔpH formation on both sides of thylakoid membranes, dissipates excess excitation energy and initiates the photoprotection adaptation mechanism, while showing that the changes between them are positively correlated (Lu 2008). Therefore, nuclides indirectly affect CEF activity and stimulate NPQ. In theory, non-flowering plants growing at high nuclide concentrations require higher CEF activity to stimulate thermal dissipation, thereby protecting PSI from photoinhibition (Huang 2012; Miyake et al. 2005). Furthermore, chlorophyll fluorescence acts as a pressure indicator (Burger et al. 2019); there may be a response relationship between nuclide concentration and changes in fluorescence indicators. Therefore, we speculate that the intensity of thermal dissipation in non-angiosperms and the capacity of CEF are primarily related to the concentration of nuclide stress.

This study measured the chlorophyll fluorescence and P700 signal and related physiological indexes from *Racomitrium japonicum* L. grown at constant light intensity soaked in four different concentrations of Sr^{2+}. This study aimed to (1) evaluate the photosynthetic fluorescence and CEF performance of moss and (2) investigate the fluorescence parameters under Sr^{2+} treatment as the response of photosynthetic fluorescence probes to different concentrations.

Materials and methods

Plant materials and treatments

In this study, the moss *R. japonicum* collected from Zhangjiajie Forest Park, Hunan Province, China P.R. was used for experiments. After rinsed repeatedly with deionized water to remove the gravels and weeds, the *R. japonicum* was cultivated in a plastic tray in a greenhouse with moderate relative humidity (70–80%), day/night temperatures (23/17 °C) and 30% full sunlight for 2 days before stressed by $^{88}Sr^{2+}$ treatment. The treatment solutions with concentration of 5, 50 and 500 mg/L were prepared with $^{88}SrCl_2{\cdot}6H_2O$. *R. japonicum* without Sr^{2+} treatment was used as control. Plant in the conical flask for 48 h. Each conical flask was about 10 g moss. All treatments were arranged according to a completely randomized design. Each treatment was in triplicates with 6 pots of moss. After cultivation in the greenhouse for 7 days, plants were used for measuring P700 redox kinetics, chlorophyll fluorescence parameters, physiological indexes and hydrogen peroxide staining.

PSI and PSII measurements

One week after Sr^{2+} treatment, we used a Dual-PAM 100 measuring system (Heinz Walz, Effeltrich, Germany) to measure chlorophyll fluorescence parameters. The light intensity used in the determination was adjusted to 1000 μmol photons m^{-2} s^{-1} before determination, and the parameters were set after full dark adaptation of 15 min. The PSI parameters were calculated as follows as follows: $Y(I) = (P_m' - P)/P_m$, $Y(ND) = P/P_m$ and $Y(NA) = (P_m - P_m')/P_m$. Y(I) represents the quantum yield of PSI photochemistry; Y(ND), the quantum yield of PSI non-photochemical energy dissipation due to the donor side limitation; Y(NA), the quantum yield of the non-photochemical energy dissipation due to the acceptor side limitation. In addition, the PSII parameters were calculated as follows (Hendrickson et al. 2004; Kramer et al. 2004): $F_v/F_m = (F_m - F_o)/F_m$, $Y(II) = (F_m' - F_s)/F_m'$, $Y(NO) = F_s/F_m$ and $NPQ = (F_m - F_m')/F_m'$, $Y(NPQ) = 1 - Y(II) - Y(NO)$, where F_o is the minimum fluorescence intensity after dark adaptation; F_m and F_m' are the maximum fluorescence intensity after dark and light adaptation, respectively; and F_s is the light-adapted fluorescence. F_v/F_m represents the maximum quantum yield of PSII; Y(II), the effective quantum yield of PSII photochemistry; Y(NO), the quantum yield of non-regulatory energy dissipation in PSII; NPQ, non-photochemical quenching in PSII, Y(NPQ), the quantum yield of regulatory energy dissipation in PSII. Furthermore, the electron transport rate through PSI (or PSII) was calculated as: ETRI (or ETRII) = PPFD × Y(I) (or Y(II)) × 0.84 × 0.5, where PPFD is photosynthetic photon flux density, and the light absorption is assumed to be 0.84 of incident irradiance. The total photosynthetic electron transport rate CEF is calculated by subtracting ETRII120s from ETRI120s and the capacity of CEF (YCEF) by subtracting Y(II) from Y(I).

Measurement of P700 redox kinetics

Before the determination, to inactivate the Calvin cycle and reduce the interference of CO_2 in the air to the experiment, we should make the moss adapt in the dark for 2 h. Then, we used the $P700^+$ measurement mode of Dual-PAM 100 measuring system to keep the dark-adapted moss under high light for at least 30 s. After that, we standardized the data to obtain that the moss was treated with 5, 50 and 500 mg/L for the first 10 s. The redox kinetics curves from dark to 1000 μmol photons m^{-2} s^{-1} were obtained. We conducted all photosynthetic measurements in a phytotron in which the relative humidity was controlled at 70%. The air temperature was controlled at a constant room temperature.

Chlorophyll content, H_2O_2, catalase and malondialdehyde analysis

Briefly, fresh leaves (0.3 g) were cut into small pieces, and then chlorophyll content, hydrogen peroxide contents, MDA and catalase contents were measured. The chlorophyll content was determined with spectrophotometry in the dark by Yanger Chen (2007) (Chen 2007). The hydrogen peroxide content of fresh plant were determined using the methods of Lv (2020) (Lv and Chng 2020). The MDA and CAT content of *R. japonicum* was determined with the thiobarbituric acid (TBA) reaction and with ultraviolet absorption method by following the procedure developed by Dhindsa (1981) (Dhindsa et al. 1981). The determination of each physiological index was repeated for 3 times, and the average value was taken.

Dyeing of hydrogen peroxide

We removed the moss root, washed them with distilled water and placed them in a 50-ml centrifuge tube. The distribution of hydrogen peroxide in leaves was marked using Zhang et al. (2009). Briefly, approximately 0.3 g of fresh sample was placed in DAB dye solution (1 mg/mL, pH3.8) and then adjusted the pH of the solution to 5.8 with sodium hydroxide (NaOH). After being stored at 28 ℃ for 8 h in the dark, we sucked out the tubes of the dye. We then extracted with 80% ethanol in boiling water until the leaves were completely discolored. Finally, we sucked out the liquid in each tube and stored it in a refrigerator at 4 ℃. For a while, we observed the distribution of hydrogen peroxide in *R. japonicum* under a microscope (Zhang et al. 2009).

Data analysis

Data were processed by Microsoft Excel (2020) and SPSS 26.0. Figures were drawn using the Graph Pad Prism 8.0 software program. Mean values based on sextuplicate were calculated. Differences between treatments were considered significant at $p < 0.05$.

Results

Effects of Sr^{2+} on PSII and PSI of *R. japonicum*

We first measured the photosynthetic efficiency upon the abrupt illumination of dark-adapted plants to assess moss responses to nuclide stimulation. After transitioning from the dark to actinic light (1000 µmol photons m^{-2} s^{-1}), the maximum photosynthetic efficiency of PSII (F_v/F_m) initially increased, then decreased within the range of concentration change (Fig. 1); however, there were significant differences

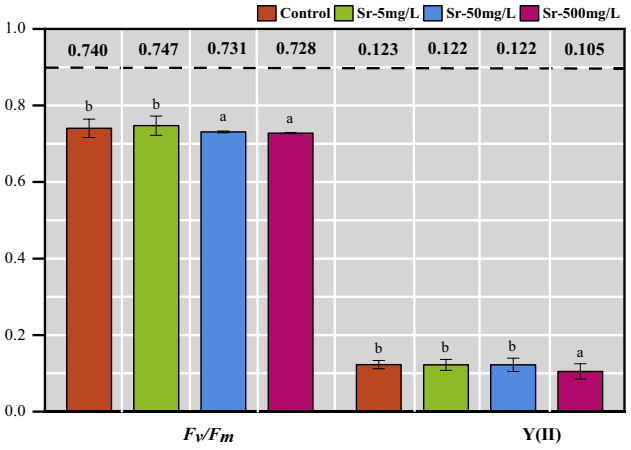

Fig. 1 The fluorescence parameter *Fv/Fm* and Y(II) in *Racomitrium japonicum* measured at 0, 5, 50, 500 mg/L strontium concentration

between the control group and the higher concentration treatment group, and the actual photosynthetic efficiency (YII) of moss after light stabilization was only different during the 500 mg/L treatment. The overall value was low (Fig. 1). The maximum photosynthetic efficiency under dark adaptation reflected the conversion efficiency of the PSII primary reaction. Under normal circumstances, F_v/F_m retained a relatively stable value, but when plants were subjected to stress, F_v/F_m decreased significantly (Dawson and Dennison 1996; Kong et al. 2016; Zhou et al. 2016). In this experiment, the maximum photochemical efficiency declined, but the actual photochemical efficiency measured after dark adaptation was not affected at low and middle Sr^{2+} levels. The conversion efficiency of light energy decreases with higher Sr^{2+} levels, stimulating the rapid electron transfer mechanism that occurs cuing light to chemical energy conversion, thus consuming considerable instantaneous electrons. In this way, the balance of relative electron transfer in plants can be achieved, and PSII damage can be reduced.

To assess the coping mechanisms after photosystem injury in the four studies, we examined PSII parameters under-treated with Sr^{2+} on 1000 µmol photons m^{-2} s^{-1} at 20 °C. After low-to-high Sr^{2+} concentration transition, the quantum yield of regulatory energy dissipation in PSII (Y(NPQ)) increased significantly (Fig. 2A), and Y(NPQ) increased more rapidly after treatment with the 500 mg/L Sr^{2+} solution than after treatment with the 5 mg/L Sr^{2+} solution. Meanwhile, the quantum yield of non-regulatory energy dissipation in PSII (Y(NO)) showed no change (Fig. 2B); however, NPQ in PSII rapidly increased (Fig. 2C). The decrease of Y(II) indicates that the light energy conversion efficiency of PSII was reduced, and the high-energy electrons emitted by the pigment molecules in the excited reaction center could not typically transfer further along the photosynthetic electron transport chain, resulting in the

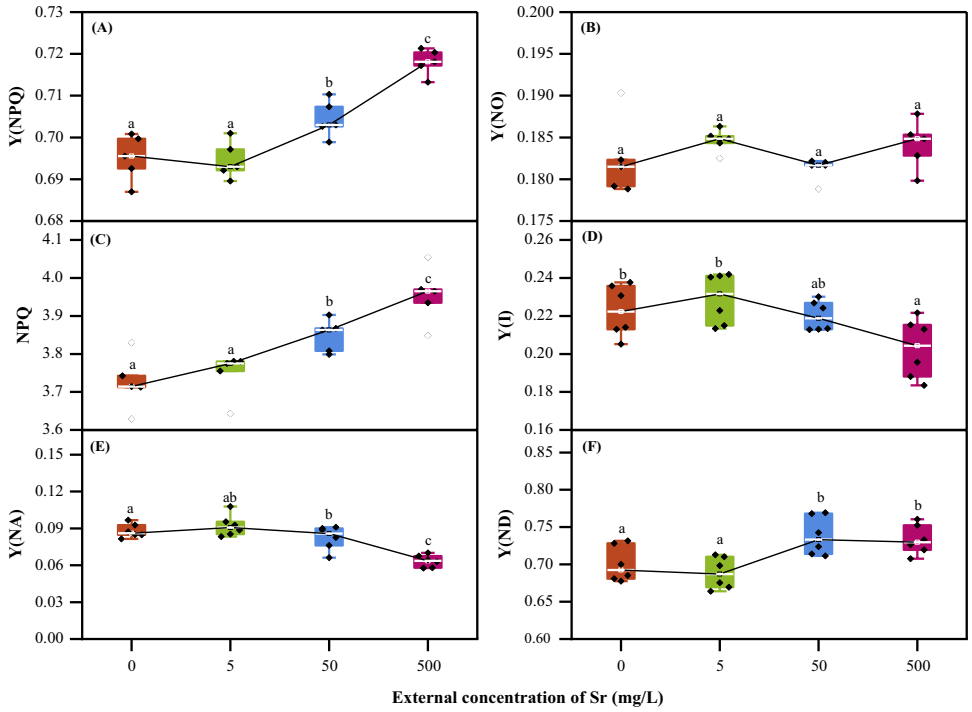

Fig. 2 The fluorescence parameter (Y(NPQ), Y(NO), NPQ, Y(I), Y(NA), Y(ND)) (**A**–**F**) in *R. japonicum* measured at 0, 5, 50, 500 mg/L strontium concentration

temporary accumulation of electrons in PSII. To alleviate the photosystem damage caused by the increase of photo quantum, the moss consumed the excess electrons via heat dissipation. Y(NO) and Y(NPQ) reflect two different forms of dissipation. From the measured data, the non-regulatory dissipation is almost unchanged, and the regulatory heat dissipation increases with strontium concentration. These results indicate that the decrease of light energy efficiency caused by strontium enhances the non-radiative dissipation (NPQ) of energy. Heat dissipation was not easily excited after strontium concentration at 5 mg/L but was sensitive to strontium concentration at 500 mg/L. In order to relieve the electronic pressure, the moss usually provides effective photoprotection in the form of active dissipation (Huang 2012).

In contrast to PSII performance under different Sr^{2+} concentrations, Sr^{2+} solution treatment significantly affected PSI performance. The quantum yield of PSI (Y(I)) has a downward trend, but the difference between adjacent concentrations was not significant (Fig. 2D). When increasing the concentration, the PSI donor-side limitation (Y(ND)) increased to its maximum values at 50 mg/L (Fig. 2E), while the PSI acceptor-side limitation (Y(NA)) shows a significant decrease under Sr^{2+} treatment (Fig. 2F). Y(I) represents the actual photochemical efficiency of PSI, while Y(ND) and Y(NA) reflect the heat dissipation effect at the donor and acceptor ends of PSI. With the increase of treatment concentration, the change of Y(I) was small, indicating that PSI was less affected; however, Y(ND) increased, indicating that the proportion of oxidation state P700 in PSI increased, and the decrease of Y(NA) reduces the risk of PSI damage (Harbinson and Foyer 1991). The high level of Y(ND) and low level of Y(NA) also suggest that cycle electron transport was an important protector in PSI. However, the level of Y(ND) was related to the linear electron blockage and was also related to the excitation of cycle electron transport (Huang 2012). Combined with PLS-DA analysis (Fig. 3A–B), it was found that there were significant differences between the 500 mg/ L Sr^{2+} treatment and the control group, especially in Y(NA) and Y(CEF), indicating that the high Sr^{2+} treatments produced stress on the mosses. The post-stress performance was primarily in the circulating electron transport around PSI and the electron capacity of the acceptor side (Huang 2012).

To further study the relationship between Sr^{2+} and fluorescence, heat dissipation and electron transport, Pearson correlation analyses were performed to determine the correlations among Sr^{2+} concentration and the *R. japonicum* photosynthetic system parameter (Table 1). The quantum yield of PSI photochemistry (YI) showed significant ($p < 0.01$) negative correlations with Sr^{2+} concentration. Meanwhile, PSI donor-side (YND) and acceptor-side (YNA) electrons exhibited significant ($p < 0.05$) positive correlations with Sr^{2+} concentration. Furthermore, when Sr^{2+} concentrations were at their highest, greater returns were observed at NPQ, which increased dependence on the concentration and showed significant ($p < 0.01$) positive correlations with the changing concentration. After Sr^{2+} solution treatment, PSI was responsive, and electron transfer values and the values of NPQ were obvious, showing extremely significant correlation ($p < 0.01$), indicating that the heat dissipation

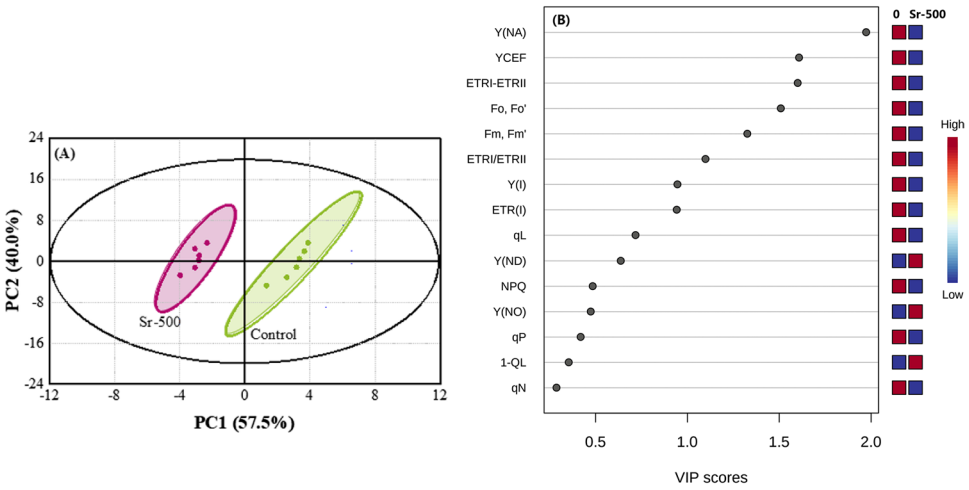

Fig. 3 The chlorophyll fluorescence parameters (**A** and **B**) responded to principal component analysis and fluorescence parameter proportion distribution of different concentrations of strontium *in R. japonicum*

Table 1 The Pearson correlation coefficients between different concentrations of strontium solutions and various fluorescence parameters

		$^{88}Sr^{2+}$	YI	YND	YNA	YII	NPQ	YCEF	ETRI-ETRII
Sr	$^{88}Sr^{2+}$	1							
PSI	Y(I)	−0.889**	1						
	Y(ND)	0.614*	−0.262	1					
	Y(NA)	0.581*	−0.527	0.571	1				
PSII	Y(II)	−0.165	0.517	−0.569	−0.254	1			
	NPQ	0.709**	−0.586*	0.271	0.424	−0.172	1		
ETR	YCEF	−0.875**	0.715**	−0.764**	−0.807**	0.231	−0.713**	1	
	ETRI-ETRII	−0.874**	0.713**	−0.759**	−0.808**	0.229	−0.715**	1.000**	1

* and * * represent significant correlations at $p < 0.05$and $p < 0.01$ levels, respectively

and electron transport in PSII were very sensitive to the change of Sr^{2+} concentration. The parameters related to electron transport ((YCEF)(ETRI-ETRII)) showed significant ($p < 0.01$) negative correlations with Sr^{2+} concentration, indicating that Sr^{2+} stimulated cycle electron transport around PSI and the induced ΔpH activated NPQ, thus consuming excessive light energy in PSII and reducing light damage (Yang et al. 2019).

Effects of Sr^{2+} on photosynthetic electron transport in *R. japonicum*

The damage mechanism of the light reaction center showed that the excitation of cycle electrons was essential to the response of the moss to Sr^{2+} stress. To assess the role of cycle electrons in electron transport, we calculated the cycle electron transfer rate of PSI reaction center by subtracting $ETRII_{120s}$ from $ETRI_{120s}$. As shown in Fig. 4A, after

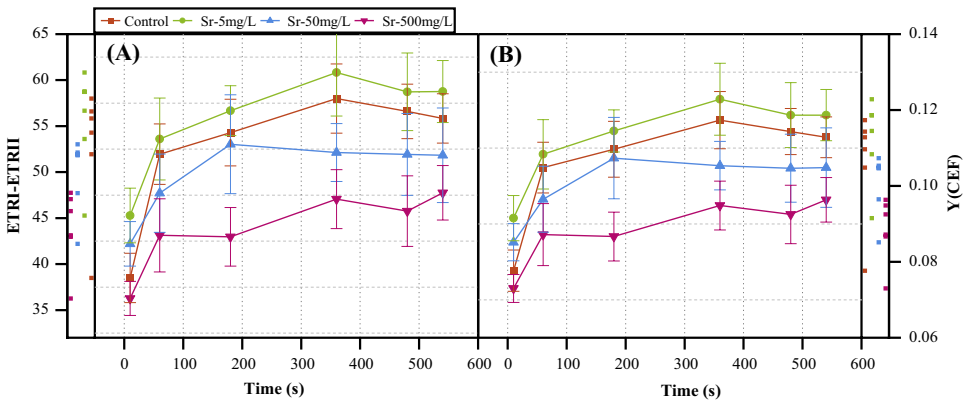

Fig. 4 The rate (ETRI-ETRII) (**A**) and size (YCEF) of electron transfer (**B**) in *R. japonicum* measured at 0, 5, 50, 500 mg/L strontium concentration

concentration intensity increases, the ETRI-ETRII rapidly increased in the first 10 s and remained stable after 1 min. The initial increase in ETRI-ETRII was attributed mainly to the stimulation of Sr^{2+} concentration, and the subsequent stable state was mainly attributed to the regulation of electron transport pathways. These results indicate that the cyclic electron transport decreased with increasing concentration, but ETRI-ETRII can be excited at low levels with a high concentration solution. Notably, the same trend applied to the CEF capacity, which was calculated by Y(I)-Y(II). The CEF decreased significantly with a 500 mg/L Sr^{2+} concentration, but increased with a 5 mg/L Sr^{2+} concentration, when considering average plant growth (Fig. 4B). Combined with the rate of cycle electron transfer, the absolute electron transfer rate showed the same trend, highlighting the positive response mechanism of CEF exposed to low concentration in moss. When a high Sr^{2+} concentration entered the moss, the electron transfer of the photosystem was under certain pressure, the capacity of PSI receiving electrons was reduced, and the rate of electron transfer was slowed, seriously hindering the standard transmission of linear electrons. This stress makes it easy to excite circulating electrons at high concentrations, showing an instantaneous rise and then reaching a relatively stable trend, and the stabilized electron transport depended on the energy distribution between PSI and PSII.

To examine the influence of energy distribution on CEF and the contribution of CEF to the total electron flow, we compared the Y(I)/Y(II) ratios in mosses at different Sr^{2+} concentration (Fig. 5A). With increasing concentration, the Y(I)/Y(II) ratio increased, stabilized, then declined, and the Y(I)/Y(II) ratio at 50 and 500 mg/L Sr^{2+} concentrations were significantly lower than that of the 5 mg/L treatment. Furthermore, Y(I)/Y(II) values at low light (59 µmol photons m^{-2} s^{-1}) were more significant than 1, highlighting the total current decreased significantly at a high concentration of Sr^{2+} stress, affecting the energy distribution of PSI and PSII, and more light was absorbed in PSII, which was consumed in the form of active dissipation. Based on the regression analyses between the degree of cyclic electron excitation and the degree of PSI damage under 500 mg/L Sr^{2+} stress (Fig. 5B), a linear positive correlation between YCEF and YI under high concentration (500 mg/L) Sr^{2+} stress was found, pointing to the cyclic electron transfer as being closely related to PSI in the *R. japonicum* under Sr^{2+} stress, which causes the total current to decrease and the linear electrons to be blocked. The cycle electron transport pathway plays an important role in ensuring the regular operation of electrons. Additionally, the changing trend of total electron flow is consistent with that of annular electron flow, suggesting that the cyclic electron transfer accounts for a large part of the distribution of the total electron flow.

The important role of the cycle electron pathway is that the electrons are rapidly consumed by oxidation in PSI, thus avoiding the harm caused by electron accumulation to the photosystem. The path of electron oxidation depends on the response of FLV in the pseudo-cyclic electron transport path. To determine the response of FLV-dependent flow to treatment concentration, we examined the P700 redox kinetics of the moss after Sr^{2+} treatment (Fig. 6). After the transition from dark to actinic light (1000 µmol photons m^{-2} s^{-1}), the mosses initially oxidized and then reduced, then oxidized again and stabilized. The P700 reduction reflects the electron flow to PSI originating from water splitting at PSII (Alboresi et al. 2019; Huang et al. 2019b), and the final re-oxidation of P700 non-angiosperms was attributed to O_2 photo-reduction mediated by FLVs or water-water cycle (Sun et al. 2020; Shikanai and Yamamoto 2017; Tan et al. 2020b). *R. japonicum* displayed the fast re-oxidation of P700 in approximately 2 s after the transition from dark to actinic light, indicating the role of FLVs under the electron transfer pathway. As

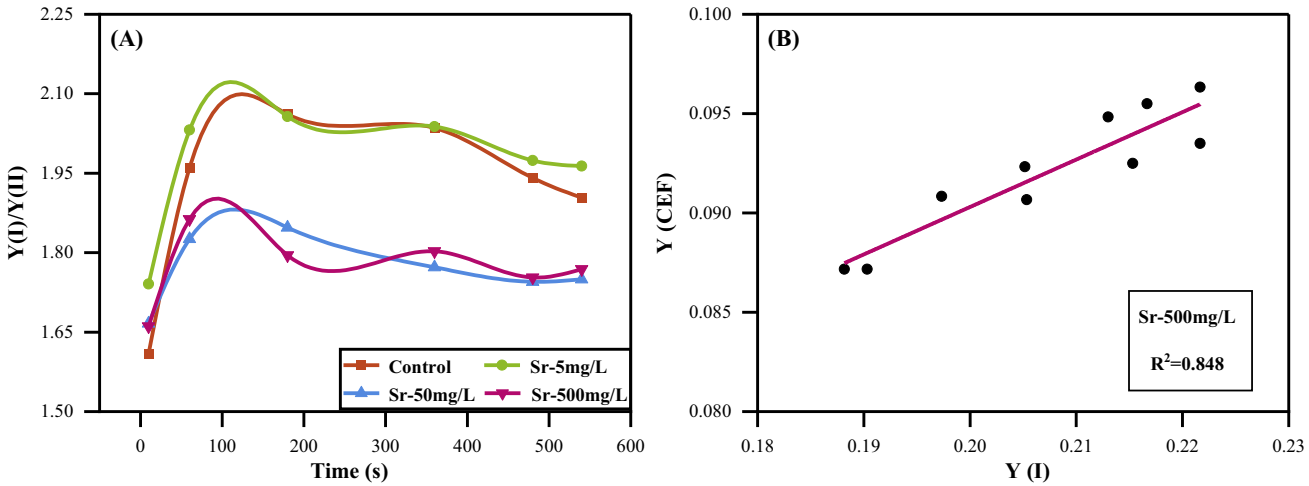

Fig. 5 The Y(I)/Y(II) ratio (**A**) and the correlation of YCEF and YI (**B**) in *R. japonicum* measured at 0, 5, 50, 500 mg/L strontium concentration

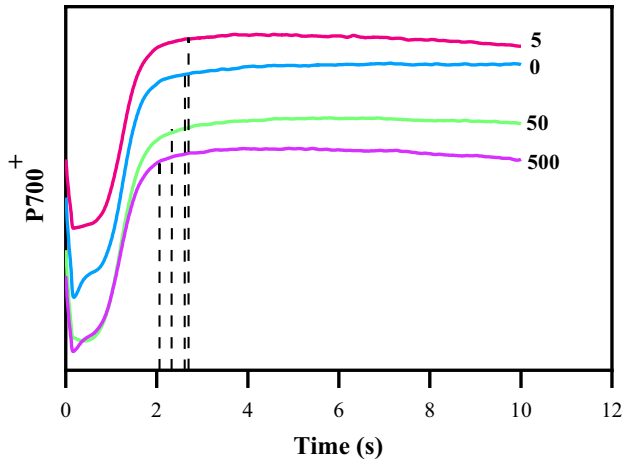

Fig. 6 The redox kinetics of P700 upon transition from dark to actinic light (1000 µmol photons m^{-2} s^{-1}) in *R. japonicum* measured at 0, 5, 50, 500 mg/L strontium concentration. All data are means of nine independent experiments

shown in Fig. 6, the reduction and final re-oxidation of P700 occurred much more quickly at 50 and 500 mg/L than at 5 mg/L, indicating that water splitting and FLV activities were largely inhibited at 5 mg/L, but were upregulated at 50 and 500 mg/L.

Effects of Sr^{2+} on chlorophyll a/b, H_2O_2, MDA and CAT in *R. japonicum*

The Sr^{2+} concentration stimulations can change the content of some substances in cells. The chlorophyll-a/b concentrations increased before decreasing with increased Sr^{2+} stress (Fig. 7A). Compared to the control check group, the high concentration group had a significant decrease in chlorophyll a/b (Li et al. 2019). The chla/b ratio of typical shade plants is about 2.3 (Chen 2007), while under 50 and 500 mg/L Sr^{2+} treatment, this ratio was much lower than the average value, at approximately 0.8. The difference between the control check group and the Sr^{2+} treatment groups can be credited to the toxicity stress caused by Sr^{2+} (Li et al. 2019). With the decrease of Chla content, the ability to convert light energy into biochemical energy decreased, which indirectly increased reactive oxygen species. Furthermore, according to Fig. 8, the H_2O_2 content in *R. japonicum* decreased significantly at 5 mg/L Sr^{2+} concentration and gradually increased at 50 and 500 mg/L. This is also supported by staining and locating the H_2O_2 content in moss (Fig. 8), indicating that the distribution of H_2O_2 was less at 5 mg/L strontium concentration; however, when treated with Sr^{2+} at 50 and 500 mg/L, H_2O_2 was distributed on the stem and leaf edge of *R. japonicum*, and with most of them showing punctate distribution of stem. Meanwhile, under a high concentration of Sr^{2+} stress, the content of MDA (Fig. 7C), the product of membrane lipid peroxidation increased, inducing cell damage and oxidative stress resistance to the enzyme system of the organism. For CAT (Fig. 7B), the trend followed the same trend as H_2O_2 changes. Furthermore, we observed that the treatment groups with high CEF rates showed increasing production of hydrogen peroxide.

Discussion

Photosynthetic fluorescence response of moss under Sr^{2+} stress

Chlorophyll fluorescence parameters can be used to elucidate the mechanism of tolerance of the *Barbula subcontorta* Broth. and *Marchantia polymorpha* L. to Pb^{2+} in the environment and can be used as a rapid method to identify and judge the pollution resistance of bryophytes (Zhang et al. 2011). Little is known about the response

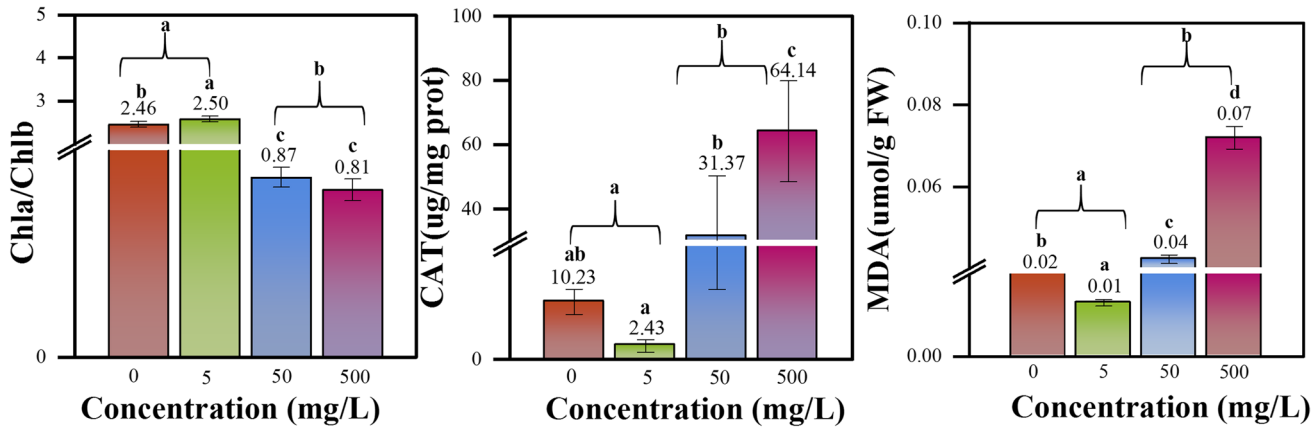

Fig. 7 The concentrations of chlorophyll-a/b(chla/chlb), catalase (CAT), malondialdehyde (MDA) (**A**–**C**) in *R. japonicum* measured at 0, 5, 50, 500 mg/L strontium concentration

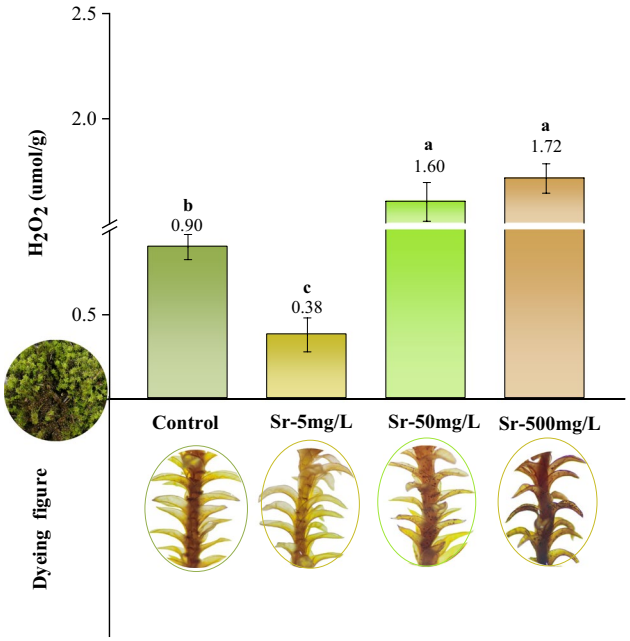

Fig. 8 The proportion diagram of hydrogen peroxide (H_2O_2) content and the staining location map of H_2O_2 content in *R. japonicum* measured at 0, 5, 50, 500 mg/L strontium concentration

of photosynthetic fluorescence in mosses to nuclide treatment. We examined the chlorophyll fluorescence parameters of moss under Sr^{2+}. At the concentration of 5 mg/L, the primary light energy conversion efficiency (F_v/F_m) and photochemical quantum yield (YII) of PSII decreased, and NPQ and donor-side restriction Y (ND) increased with the increase of Sr^{2+} concentration (Figs. 1 and 2). Since the decrease in F_v/F_m and (YII) was predominantly attributed to the decrease in light energy conversion efficiency, this finding suggests that photosynthetic fluorescence of the moss was stimulated at lower concentrations and inhibited at higher concentrations. Y(NPQ) and NPQ are responsible for consuming excess electrons in PSII. When the Sr^{2+} concentration increased to 50 mg/ L, the value of NPQ was significantly higher than that of 5 mg/ L, indicating that the heat dissipation in PSII increased rapidly at higher Sr^{2+} concentrations (Fig. 2). NPQ is a rapidly switchable mechanism by dissipating the excess absorbed energy as heat, which is triggered by the pH gradient across the thylakoid membrane and requires the protein PsbS and the xanthophyll zeaxanthin. Nicol et al. (2019) recently reported that PsbS-dependent NPQ occurs mainly in LHCII (approximately 60%), and the remaining 40% quenching site in the PSII core. Therefore, the drastic photoinhibition of PSII might result from the significant decrease in NPQ (Fig. 2), as well as the degradation of chlorophyll complexes (Nicol et al. 2019). The Plsda and correlation analysis showed significant difference between high concentration Sr^{2+} concentrations and the control group, and the circulating electron transfer and heat dissipation were significantly correlated with Sr^{2+} concentration. The concentration of 500 mg/L caused damage to the photosystem and reduces the photosynthetic conversion efficiency. The increased electron flow from PSII must be rapidly consumed in the form of heat dissipation to accelerate the electron transfer rate to PSI and prevent the excessive accumulation of electrons in PSI. Therefore, the light response of photosynthetic fluorescence under Sr^{2+} stress is tightly linked to the electron transport rate and heat dissipation.

Several studies on *Barbula subcontorta* Broth. suggested that the NPQ and ETR_{max} increased first and then decreased (Zhang et al. 2011). However, in this study, with an increase of Sr^{2+} concentration, NPQ decreased at low concentrations but increased at high concentrations, indicating that the way of consuming excess electrons is primarily via active dissipation of the photosystem. As the value of NPQ changes significantly at 500 mg/L, heat dissipation is instrumental in the pathway of excessive electron consumption. These results suggested that heat dissipation in the moss is strongly influenced by the stimulation of high Sr^{2+} concentration, and the chlorophyll fluorescence parameter NPQ can be used as a fluorescent probe for the photosynthesis of the moss under Sr^{2+} stress. Furthermore, the circulating electron transport pathway is another effective way to transfer excess electrons.

CEF response of moss under strontium stress

In the study of drought stress in *Paraboea sinensis*, the cycle electron transfer was able to upregulate to more than three times of the linear electron transfer, which was crucial to light energy conversion and photoprotection (Huang 2012); however, the nuclide responses of CEF in moss were poorly understood. In this study, ETRI-ETRII can be excited at a low level in a high concentration solution (Fig. 4), but CEF decreases with the increase of concentration. Meanwhile, there was a positive correlation between the excitation of cycle electrons and the degree of PSI damage (Fig. 4), which made it possible for the moss to avoid PSI damage by the way of cycle electrons. Furthermore, at high concentrations (50 mg/L and 500 mg/L), FLV activity was quickly upregulated, oxidizing excess photoelectrons in PSI and achieving rapid light energy conversion. Initial CEF stimulation promoted the rapid formation of ΔpH and prevented uncontrolled light damage to PSI (Yamamoto and Shikanai 2019). The subsequent reduction of CEF prevents excessive acidification of the thylakoid lumen, thus optimizing the trade-off between photoprotection and photo utilization efficiency (Tan et al. 2021; Yang et al. 2019). Here, the concentrations of 50 and 500 mg/L stimulated the excitation of cycle electrons. The electrons inhibited in the linear electron path can reach the electron equilibrium

through CEF. The improvement of FLV activity accelerates the electron oxidation and synergizes with CEF to optimize the balance between photoprotection and photo utilization efficiency. This is consistent with previous works by Lei et al. (2021) on photosynthetic regulation of light environment changes under temperature stress of moss.

Conclusions

This study examined photosynthetic regulation under different Sr^{2+} concentrations in *R. japonicum*. Moderate and high Sr^{2+} stress induced photo-inhibition and photo-damage in PSI and PSII of *R. japonicum.* The electrons absorbed by the pigment antenna were consumed in PSII primarily via active dissipation YNPQ. The increase of NPQ had a significant synergistic effect with the change of Sr^{2+} concentration; therefore, this fluorescence probe could be potential to monitor the Sr^{2+} stress. After stimulated by Sr^{2+} stress, the cycle electrons play an indispensable role. The electrons accumulated in PSI may get the balance of photosynthetic protection and rapid photoelectron conversion by stimulating CEF and increasing FLV activity. Thus, the photosynthetic acclimation to Sr^{2+} stress at different concentration in moss *R. japonicum* is linked to the adjustment of FLVs and CEF.

Author contribution All authors contributed to the study conception and design. KC, RHH and YBL conceived and designed research. HR and YHL conducted experiments. RHH, WTL, LLZ and HR analyzed data. HR, KC and YBL wrote the first draft of the manuscript and intensively edited by all authors.

Funding This work was supported by the National Key Research and Development Program of China (2020YFE0203200), the Open Fund Program of the CAS Key Laboratory of Mountain Ecological Restoration and Bioresource Utilization and Ecological Restoration and Biodiversity Conservation Key Laboratory of Sichuan Province, Chengdu Institute of Biology, Chinese Academy of Sciences (KXYSWS2204), Sichuan Science and Technology Department Program (2020YFS0344, 2022YFS0492, 2021YFH0008, 2022YFH0040) and the Opening Project of Hubei Engineering Research Center for Specialty Flowers Biological Breeding (2022ZD003).

Data availability The datasets analyzed during this study are available from the corresponding author.

Declarations

Ethics approval This article does not contain any studies with human participants or animals performed by any of the authors.

Consent for publication All authors whose names appear on the submission approved the version to be published and agree to be accountable for all aspects of the work in ensuring that questions related to the accuracy or integrity of any part of the work are appropriately investigated and resolved.

Conflict of interest The authors declare no competing interests.

References

Alboresi A, Storti M, Morosinotto T (2019) Balancing protection and efficiency in the regulation of photosynthetic electron transport across plant evolution. New Phytol 221(1):105–109

Brestic M, Zivcak M, Kunderlikova K, Allakhverdiev SI (2016) High temperature specifically affects the photoprotective responses of chlorophyll b-deficient wheat mutant lines. Photosynth Res 130(1):251–266

Brestic M, Zivcak M, Kunderlikova K, Sytar O, Shao H, Kalaji HM, Allakhverdiev SI (2015) Low PSI content limits the photoprotection of PSI and PSII in early growth stages of chlorophyll b-deficient wheat mutant lines. Photosynth Res 125(1):151–166

Burger A, Weidinger M, Adlassnig W, Puschenreiter M, Lichtscheidl I (2019) Response of *Plantago major* to cesium and strontium in hydroponics: absorption and effects on morphology, physiology and photosynthesis. Environ Pollut 254:113084

Chen Y-E (2007) Determination of heavy metal content in bryophytes and effects of heavy metal stress on physiological indexes of bryophytes. Doctoral dissertation of SichuanUniversity, Chengdu

Cheng X, Chen C, Hu Y, Guo X, Wang J (2022a) Photosynthesis and growth of *Amaranthus tricolor* under strontium stress. Chemosphere 308:136234

Cheng X, Chen C, Hu Y, Wang J (2022b) Response of *Amaranthus tricolor* to cesium stress in hydroponic system: growth, photosynthesis and cesium accumulation. Chemosphere 307:135754

Choppin G (2007) Actinide speciation in the environment. J Radioanal Nucl Chem 273(3):695–703

Dawson S, Dennison W (1996) Effects of ultraviolet and photosynthetically active radiation on five seagrass species. Mar Biol 125(4):629–638

Dhindsa RS, Plumb-Dhindsa P, Thorpe TA (1981) Leaf senescence: correlated with increased levels of membrane permeability and lipid peroxidation, and decreased levels of superoxide dismutase and catalase. J Exp Bot 32(1):93–101

Harbinson J, Foyer CH (1991) Relationships between the efficiencies of photosystems I and II and stromal redox state in CO_2-free air: evidence for cyclic electron flow in vivo. Plant Physiol 97(1):41–49

Hendrickson L, Furbank RT, Chow WS (2004) A simple alternative approach to assessing the fate of absorbed light energy using chlorophyll fluorescence. Photosynth Res 82(1):73–81

Huang W (2012) Cycle electron transport plays an important role in plant resistance to environmental stress. University of Science and Technology of China, Hefei

Huang W, Yang Y-J, Zhang S-B (2019a) Photoinhibition of photosystem I under fluctuating light is linked to the insufficient ΔpH upon a sudden transition from low to high light. Environ Exp Bot 160:112–119

Huang W, Yang Y-J, Zhang S-B (2019b) The role of water-water cycle in regulating the redox state of photosystem I under fluctuating light. Biochimica et Biophysica Acta (BBA)-Bioenergetics 1860 (5):383–390

Kong F, Liu X-Y, Wang G-Z, Zhang K (2016) Effects of fertilizer dosage on photosynthesis and fast chlorophyll fluorescence characteristics of *Juglans regia* in mountainous region. For Res 29(5):764

Kramer DM, Johnson G, Kiirats O, Edwards GE (2004) New fluorescence parameters for the determination of QA redox state and excitation energy fluxes. Photosynth Res 79(2):209–218

Lai J-l, Luo X-g (2019) High-efficiency antioxidant system, chelating system and stress-responsive genes enhance tolerance to cesium ionotoxicity in Indian mustard (*Brassica juncea* L.). Ecotoxicol Environ Saf 181:491–498

Li C, Wang M, Luo X, Liang L, Han X, Lin X (2019) Accumulation and effects of uranium on aquatic macrophyte *Nymphaea*

tetragona Georgi: potential application to phytoremediation and environmental monitoring. J Environ Radioact 198:43–49
Li H, Tang Y-J, Zeng F (2013) Effects of high concentration Strontium and Cesium stress on chlorophyll fluorescence characteristics of plants. Jiangsu Agri Sci 41(9):349–352
Li Z, Wakao S, Fischer BB, Niyogi KK (2009) Sensing and responding to excess light. Annu Rev Plant Biol 60:239–260
Lu K-S (2008) Effects of salt stress on photosynthesis and antioxidant system of Soybean and its regulatory mechanism. Hangzhou: Doctoral dissertation of Zhejiang University
Luo H-Y, Gao H-B, Xia Q-P, Gong B-B, Wu X-L (2011) Effects of γ -aminobutyric acid on reactive oxygen metabolism and chlorophyll fluorescence parameters of tomato under salt stress. J Integr Agric 44(4):753–761
Lv Q-P, Chng X-A (2020) To study the changes of hydrogen peroxide and polyphenol oxidase in *Prunus eurysolis* under waterlogging stress. J Fruit Resour 1(1):1–5
Maksimovic I, Kastori R, Putnik-Delic M, Borišev M (2014) Effect of yttrium on photosynthesis and water relations in young maize plants. J Rare Earths 32(4):372–378
Marešová J, Pipíška M, Rozložník M, Horník M, Remenárová L, Augustín J (2011) Cobalt and strontium sorption by moss biosorbent: modeling of single and binary metal systems. Desalination 266(1–3):134–141
Meng X-L (2013) Photodamage defense mediated by mitochondrial alternation oxidase pathway in Cucumber leaves under different light and temperature conditions. Doctoral dissertation of Shandong Agricultural University, Taian
Miyake C, Miyata M, Shinzaki Y, Tomizawa K-i (2005) CO_2 response of cyclic electron flow around PSI (CEF-PSI) in tobacco leaves—relative electron fluxes through PSI and PSII determine the magnitude of non-photochemical quenching (NPQ) of Chl fluorescence. Plant Cell Physiol 46(4):629–637
Nicol L, Nawrocki WJ, Croce R (2019) Disentangling the sites of non-photochemical quenching in vascular plants. Nature Plants 5(11):1177–1183
Paatero J, Jaakkola T, Kulmala S (1998) Lichen (sp. Cladonia) as a deposition indicator for transuranium elements investigated with the Chernobyl fallout. J Environ Radioact 38(2):223–247
Shikanai T, Yamamoto H (2017) Contribution of cyclic and pseudo-cyclic electron transport to the formation of proton motive force in chloroplasts. Mol Plant 10(1):20–29
Shimakawa G, Miyake C (2019) What quantity of photosystem I is optimum for safe photosynthesis? Plant Physiol 179(4):1479–1485
Storti M, Alboresi A, Gerotto C, Aro EM, Finazzi G, Morosinotto T (2019) Role of cyclic and pseudo-cyclic electron transport in response to dynamic light changes in Physcomitrella patens. Plant Cell Environ 42(5):1590–1602
Strand DD, Livingston AK, Satoh-Cruz M, Froehlich JE, Maurino VG, Kramer DM (2015) Activation of cyclic electron flow by hydrogen peroxide in vivo. Proc Natl Acad Sci 112(17):5539–5544
Sun H, Yang Y-J (1861) Huang W (2020) The water-water cycle is more effective in regulating redox state of photosystem I under fluctuating light than cyclic electron transport. Biochim Biophys Acta (BBA)-Bioenerg 9:148235
Takagi D, Takumi S, Hashiguchi M, Sejima T, Miyake C (2016) Superoxide and singlet oxygen produced within the thylakoid membranes both cause photosystem I photoinhibition. Plant Physiol 171(3):1626–1634
Tan S-L, Huang J-L, Zhang F-P, Zhang S-B, Huang W (2021) Photosystem I photoinhibition induced by fluctuating light depends on background low light irradiance. Environ Exp Bot 181:104298
Tan S-L, Liu T, Zhang S-B, Huang W (2020a) Balancing light use efficiency and photoprotection in tobacco leaves grown at different light regimes. Environ Exp Bot 175:104046
Tan S-L, Yang Y-J, Huang W (2020b) Moderate heat stress accelerates photoinhibition of photosystem I under fluctuating light in tobacco young leaves. Photosynth Res 144(3):373–382
Tikkanen M, Mekala NR (1837) Aro E-M (2014) Photosystem II photoinhibition-repair cycle protects Photosystem I from irreversible damage. Biochim Biophys Acta (BBA)-Bioenerg 1:210–215
Walker BJ, Strand DD, Kramer DM, Cousins AB (2014) The response of cyclic electron flow around photosystem I to changes in photorespiration and nitrate assimilation. Plant Physiol 165(1):453–462
Wang X, Chen C, Wang J (2017) Phytoremediation of strontium contaminated soil by Sorghum bicolor (L.) Moench and soil microbial community-level physiological profiles (CLPPs). Environ Sci Pollut Res 24(8):7668–7678
Yamamoto H, Shikanai T (2019) PGR5-dependent cyclic electron flow protects photosystem I under fluctuating light at donor and acceptor sides. Plant Physiol 179(2):588–600
Yamamoto H, Takahashi S, Badger MR, Shikanai T (2016) Artificial remodelling of alternative electron flow by flavodiiron proteins in *Arabidopsis*. Nat Plants 2(3):1–7
Yamori W, Makino A, Shikanai T (2016) A physiological role of cyclic electron transport around photosystem I in sustaining photosynthesis under fluctuating light in rice. Sci Rep 6(1):1–12
Yang Y-J, Ding X-X, Huang W (2019) Stimulation of cyclic electron flow around photosystem I upon a sudden transition from low to high light in two angiosperms *Arabidopsis thaliana* and *Bletilla striata*. Plant Sci 287:110166
Zhang, G-F, Duan, Z-Z, Luo, X-J, Su, W-H (2011) Chlorophyll fluorescence characteristics and tolerance of two mosses in response to Pb^{2+} concentration. Environ Pollut Cont 1:36–40
Zhang X-L, Wang P-C, Song C-P (2009) Method for determination of hydrogen peroxide in plant cells. Journal of Plant 44(01):103
Zhou D-D, Liu D-X, Li C-H, Chen M-M, Liu G-M, Yang Q-S, Li Y-T (2016) Photosynthetic characteristics and chlorophyll fluorescence parameters of Celtis sinensis and Ulmus pumila L. seedling under salt stress. Acta Bot Boreali-Ocidentalla Sin 36(5):1004–1011
Zivcak M, Brestic M, Kunderlikova K, Sytar O, Allakhverdiev SI (2015) Repetitive light pulse-induced photoinhibition of photosystem I severely affects CO2 assimilation and photoprotection in wheat leaves. Photosynth Res 126(2):449–463